J Therm Anal Calorim (2017) 130:311–318
DOI 10.1007/s10973-017-6355-8

Reinvestigations of the Li_2O–WO_3 system

Piotr Tabero[1] · **Artur Frackowiak**[1]

Received: 1 December 2016 / Accepted: 24 March 2017 / Published online: 6 April 2017

Abstract Reinvestigations of the Li_2O–WO_3 system have been performed with the help of DTA–TG, XRD, IR and UV–Vis–NIR/DRS measuring techniques and WO_3 and Li_2CO_3 as a reactants. Results of investigations have shown that using applied procedure of synthesis four single phases have been obtained: Li_2WO_4, $Li_2W_2O_7$, α-Li_4WO_5 and β-Li_4WO_5. We failed to obtain pure samples of $Li_2W_5O_{16}$, $Li_2W_4O_{13}$ and $Li_6W_2O_9$, although diffraction reflection characteristic for these phases was identified on powder diffraction patterns of several samples. On the other hand, the formation of Li_6WO_6 has not been corroborated by XRD in our research. Results of DTA–TG investigations have revealed that phases $Li_2W_2O_7$ and Li_2WO_4 melt congruently at 735 and 745 °C, respectively, whereas α-Li_4WO_5 undergoes a phase transition to β-Li_4WO_5 at 690 °C. Results of DTA–TG and IR investigations indicate that α-Li_4WO_5 can be stabilized by a small amount of carbonate groups. Based on UV–Vis–NIR/DRS investigations, band gap energies were calculated for Li_2WO_4, $Li_2W_2O_7$, α-Li_4WO_5 and β-Li_4WO_5 and are equal to 4.35, 4.03, 4.00 and 4.12eV, respectively.

Keywords Li_2O–WO_3 system · DTA–TG · XRD · IR · UV–Vis–NIR/DRS · Band gap

✉ Piotr Tabero
ptab@zut.edu.pl

[1] Szczecin, Faculty of Chemical Technology and Engineering, Department of Inorganic and Analytical Chemistry, West Pomeranian University of Technology, Al. Piastow 42, 71-065 Szczecin, Poland

Introduction

Literature scan has shown that Li_2O–WO_3 system has been the subject of many studies [1–22]. Phases forming in this system owing to their interesting properties are potential candidates for the production of components of electrodes for lithium batteries, catalysts of oxidative coupling of light hydrocarbons, fluxes for single crystal growing, electrochromic and photochromic devices as well as neutron detectors [1–4]. Previous studies on the Li_2O–WO_3 system have revealed the formation of seven binary compounds: Li_6WO_6, Li_4WO_5, $Li_6W_2O_9$, Li_2WO_4, $Li_2W_2O_7$, $Li_2W_4O_{13}$ and $Li_2W_5O_{16}$. Synthesis of phases has been conducted in air, oxygen or dry oxygen using Li_2O/WO_3, Li_2O_2/WO_3, $LiOH/WO_3$, Li_2CO_3/H_2WO_4 and the most frequently Li_2CO_3/WO_3 mixtures. Conducted investigations enabled construction of two variants of phase diagram of the Li_2WO_4–WO_3 system [5, 6] and one of the WO_3–Li_2O system [7]. IR spectra of $Li_2W_2O_7$, Li_2WO_4, $Li_2W_4O_{13}$ Li_6WO_6 as well as α and β modifications of Li_4WO_5 are known [7, 8].

Basic crystallographic data of phases forming in the system Li_2O–WO_3 are given in Table 1.

Literature survey has shown that Li_2WO_4 forms four polymorphs: rhombohedral Li_2WO_4-I, of phenacite structure and stable at atmospheric pressure, tetragonal Li_2WO_4-II obtained at 300 MPa, an orthorhombic Li_2WO_4-III, prepared above 300 MPa and at higher temperature than Li_2WO_4-II and monoclinic Li_2WO_4-IV stable at pressure higher than Li_2WO_4-III [9–12]. Crystal structures of rhombohedral, tetragonal and monoclinic structures of Li_2WO_4 were solved [9, 10, 13]. Li_2WO_4 melts at 738 °C [14] 740 °C [7, 11] or 742 °C [6]. If it is heated to well above its melting point at atmospheric pressure, some loss of Li_2O occurs by evaporation, yielding a mixture of $Li_2W_2O_7$ and Li_2WO_4 [11].

Table 1 Basic crystallographic data of phases forming in the Li_2O–WO_3 system, where CS—crystal system, 3—triclinic, M—monoclinic, O—orthorhombic, R—rhombohedral, T—tetragonal, H—hexagonal, C—cubic

Formula	Li_2O/% mol	CS	Space group	Unit cell parameters						References
				a/nm	b/nm	c/nm	α/°	β/°	γ/°	
$Li_2W_5O_{16}$	16.67	–	–	–	–	–	–	–	–	[5]
$Li_2W_4O_{13}$	20.00	–	–	–	–	–	–	–	–	[18]
$Li_2W_2O_7$	33.33	3	P-1	0.8280	0.7050	0.5040	85.40	102.13	110.29	[19]
Li_2WO_4	50.00	O	–	1.0124	1.1686	1.0071	90.00	90.00	90.00	[12]
		O	–	0.5063	1.0076	1.1610	90.00	90.00	90.00	[21]
		O	–	0.5940	0.9730	0.4970	90.00	90.00	90.00	[12]
		T	141/amd	1.1941	1.1941	0.8409	90.00	90.00	90.00	[11]
		M	C2/c	0.9755	0.5946	0.4993	90.00	90.56	90.00	[10]
		R	R-3	1.4361	1.4361	0.9603	90.00	90.00	120.00	[13]
$Li_6W_2O_9$	60.00	C	Pm-3 m	0.8310	0.8310	0.8310	90.00	90.00	90.00	[17]
Li_4WO_5	66.67	C	–	0.8290	0.8290	0.8290	90.00	90.00	90.00	[15]
		C	–	0.4150	0.4150	0.4150	90.00	90.00	90.00	[20]
		O	–	2.4700	0.8780	2.8900	90.00	90.00	90.00	[15]
		3	P-1	0.5109	0.7716	0.5061	101.80	101.78	108.77	[22]
Li_6WO_6	75.00	O	–	0.7410	0.7790	0.8880	90.00	90.00	90.00	[15]
		O	Immm	0.8902	0.2879	0.4090	90.00	90.00	90.00	[16]

Li_6WO_6 has been obtained as a result of the reaction of Li_4WO_5 with Li_2O at 500 °C or LiOH with WO_3 at 700 °C in dry oxygen [15, 16]; however, Lv and co-workers [4] failed to obtain this phase. At high temperature, Li_6WO_6 has homogeneity range, and below 440 °C, it decomposes into Li_2O and Li_4WO_5 [7]. Reau and co-workers have shown in contrast that it decomposes at 1000 °C yielding β-Li_4WO_5 and volatile Li_2O [15]. Crystal structure of orthorhombic Li_6WO_6 has been solved by Hauck [16].

Another phase forming in the system Li_2O–WO_3, $Li_2W_5O_{16}$, melts incongruently at 820 °C [4, 5, 17], whereas $Li_2W_4O_{13}$ melts incongruently at 805 °C [6], 800 °C [7, 13] or at 750 °C [18] with the deposition of $Li_2W_2O_7$ and WO_3 [18].

Pistorius [11] has found that $Li_2W_2O_7$ undergoes to sharp and reversible phase transition at 666 °C with a large latent heat. This phase melts congruently at 660 °C [18], 745 °C [5–7] or 754 °C [13]. Crystal structure of $Li_2W_2O_7$ was solved by Okada and co-workers [19].

Permentier and co-workers [17] conducing synthesis in the temperature range of 450–500 °C have obtained $Li_6W_2O_9$. According to Authors, $Li_6W_2O_9$ decomposes at 550 °C with the formation of Li_2WO_4 and β-Li_4WO_5.

Literature survey has shown that Li_4WO_5 forms two polymorphic modifications: low-temperature modification, crystallizing in cubic system α-Li_4WO_5 and high-temperature modification, crystallizing in triclinic or orthorhombic system β-Li_4WO_5 [7, 15, 20, 22]. At 690 °C, α-Li_4WO_5 undergoes to phase transition to β-Li_4WO_5 [7, 15]. According to Hauck [7], β-Li_4WO_5 melts at 1350 °C, but Rau and co-workers [15] have shown that it decomposes at 1100 °C yielding Li_2WO_4 and volatile in these conditions Li_2O. α-Li_4WO_5 can be obtained in different degrees of order–disorder depending on temperature and time of synthesis [7]. Ordered form obtained at higher temperature cannot be transferred to disordered form by heating at lower temperatures. Blasse suggests that cubic modification has disordered rock salt structure [20].

Above-presented literature survey has shown that despite numerous works published, until now there are still controversies concerning the number and composition of forming phases and conditions of their synthesis. The aim of this work was to verify literature data on Li_2O–WO_3 system.

Experimental

The following materials were used for the research: WO_3, 99.9% (Fluka AG, USA), and Li_2CO_3, a.p. (POCh, Poland).

For the experiments, seven samples were selected with contents corresponding to $Li_2W_5O_{16}$, $Li_2W_4O_{13}$, $Li_2W_2O_7$, Li_2WO_4, $Li_6W_2O_9$, Li_4WO_5 and Li_6WO_6. They represented all described in literature phases forming in the system Li_2O–WO_3. Mixtures of Li_2CO_3 and WO_3 weighed

in suitable proportions enabling preparation of 5 g of final product were homogenized in an agate mortar and calcinated at 450, 500, 550, 600, 650 and 700 °C in 24-h stages in an air atmosphere. After each heating stage, the samples were cooled down to room temperature with furnace, powdered in mortar and examined with the help of XRD. The pure phases obtained in this work were examined additionally by the DTA–TG, UV–Vis–IR/DRS and IR methods. These measuring methods were selected because they allow determination of phase composition of samples, establishing their melting temperatures as well as melting behaviour [23–30].

X-ray phase analysis (XRD) of the samples was performed using an Empyrean II diffractometer (PANalytical, The Nederlands, copper radiation filtered with a graphite monochromator) with the help of Highscore + software (PANalyticak, The Nederlands) and PDF4 + ICDD database.

The DTA–TG examinations were made with the aid of an apparatus of Paulik–Paulik–Erdey type (MOM, Hungary). Samples of 500 mg were investigated in air up to the 1000 °C at the heating rate of 10 °C min^{-1} using quartz crucibles.

The IR spectra were registered by Specord M80 spectrometer (Carl Zeiss, Jena, Germany) in the wavenumber region of 1500–200 cm^{-1} using halide discs technique (pellets in KBr at a mass ratio 1:300).

The NIR/DRS measurements were performed using a Jasco V670 spectrometer matched with integrating sphere PIN 757 (Jasco, Japan) with Spectralon as a reference material.

Results and discussion

Samples obtained after consecutive stage of heating have been subjected to XRD investigations. Results of X-ray phase analysis are given in Table 2. Analysis of data presented in Table 2 shows that in all cases synthesis starts at 450 °C, but is very slow at this temperature. Moreover, syntheses processes are complex and run with formation of several intermediates. Only in the case of $Li_2W_2O_7$, Li_2WO_4, α-Li_4WO_5 and β-Li_4WO_5 obtained samples were single phase. In accord with literature data [7, 15] in the temperature range of 650–700 °C, α-Li_4WO_5 undergoes to phase transition to high-temperature modification, β-Li_4WO_5. We failed to obtain pure samples of $Li_2W_5O_{16}$, $Li_2W_4O_{13}$ and $Li_6W_2O_9$, although diffraction reflection characteristic for these phases was identified on powder diffraction patterns of several samples. It was very characteristic for $Li_6W_2O_9$, whose diffraction reflections have been detected on diffraction patterns of all samples. On the other hand, the formation of Li_6WO_6 has not been corroborated by XRD in our research. We have encountered some problems with X-ray phase analysis of investigated samples. The lack of structural data in the cases of $Li_2W_5O_{16}$, $Li_2W_4O_{13}$, α-Li_4WO_5 and poor-quality X-ray data in some other cases makes X-ray phase analysis in the Li_2O–WO_3 system very difficult.

Powder diffraction patterns of single-phase samples of $Li_2W_2O_7$, Li_2WO_4, α-Li_4WO_5 and β-Li_4WO_5 were

Table 2 Results of X-ray phase analysis after consecutive stages of heating, where Li—Li_2CO_3, W—WO_3, O4—Li_2WO_4, α—α-Li_4WO_5, β—β-Li_4WO_5, O6—Li_6WO_6, O7—$Li_2W_2O_7$, O9—$Li_6W_2O_9$, O13—$Li_2W_4O_{13}$, O16—$Li_2W_5O_{16}$, X—unknown phase

Phase	Li_2O/% mol	Products detected after heating stage at temperature/°C					
		450	500	550	600	650	700
$Li_2W_5O_{16}$	16.67	O4	O4	O4	O7	O7	O13
		O7	O7	O7	O13	O13	O16
		O9	O9	O13	Li	Li	X
		Li	Li	Li	W	W	
		W	W	W			
$Li_2W_4O_{13}$	20.00	O4	O4	O4	O7	O7	O7
		O7	O7	O7	O13	O13	O13
		O9	O9	O13	Li	Li	O16
		Li	Li	Li	W	W	X
		W	W	W			
$Li_2W_2O_7$	33.33	O4	O4	O4	O4	O7	O7
		O7	O7	O7	O7		
		O9	O9	O9			
		Li	Li	W			
		W	W				
Li_2WO_4	50.00	O4	O4	O4	O4	O4	O4
		O7	O7	O7	O7		
		O9	O9	O9			
		Li	Li				
		W	W				
$Li_6W_2O_9$	60.00	O4	O4	O4	O4	O4	O4
		O7	O7	α	α	α	β
		O9	O9	Li	Li		
		Li	Li	O9			
		W	W				
Li_4WO_5	66.67	O4	O4	O4	O4	α	β
		O7	O7	O7	O7		
		O9	O9	O9	O9		
		Li	Li	Li	Li		
		W	α	α	α		
Li_6WO_6	75.00	O4	O4	O9	O9	Li	Li
		O7	O7	Li	Li	α	β
		O9	O9	α	α		
		Li	Li				
		W					

Table 3 Unit cell parameters and volumes of Li_2WO_4, $Li_2W_2O_7$, α-Li_4WO_5, β-Li_4WO_5 phases obtained in this work

No.	Formula	a/nm	b/nm	c/nm	α/°	β/°	γ/°	V/nm^3
1	Li_2WO_4	1.437 6(1)	1.4376 (1)	0.9616 (1)	90.00	90.00	120.00	1.7211
2	$Li_2W_2O_7$	0.8293 (4)	0.7058 (3)	0.5057 (6)	85.20 (5)	102.28 (7)	110.37 (6)	0.2711
3	α-Li_4WO_5	0.4167 (1)	0.4167 (1)	0.4167 (1)	90.00	90.00	90.00	0.0724
4	β-Li_4WO_5	0.5136 (1)	0.7755 (1)	0.5086 (1)	101.60 (2)	101.53 (2)	108.50 (2)	0.1804

Table 4 Result of indexing of X-ray powder diffraction pattern of the triclinic β-Li_4WO_5 obtained in this work

Lp.	d_{exp}/nm	d_{calc}/nm	(hkl)	100 I	Lp.	d_{exp}/nm	d_{calc}/nm	(hkl)	100 I
1	2	3	4	5	1	2	3	4	5
1	0.70474	0.70503	010	3	18	0.23909	0.23887	002	10
2	0.48036	0.48035	–110	100	19	0.23733	0.23731	1–31	2
3	0.46708	0.46701	100	5	20	0.23500	0.23501	030	3
4	0.46130	0.46115	0–11	30	21	0.23348	0.23351	200	6
5	0.39463	0.39464	−101	16	22	0.23043	0.23057	0–22	3
6	0.35659	0.35668	−111	11	23	0.22352	0.22356	−221	5
7	0.35243	0.35252	020	31	24	0.21095	0.21092	−2–11	16
8	0.33597	0.33596	110	18	25	0.20937	0.20929	−1–22	24
9	0.33252	0.33247	0–21	7	26	0.20659	0.20661	2–21	3
10	0.32318	0.32325	1–11	12	27	0.20429	0.2043	1–22	20
11	0.29459	0.29473	101	5	28	0.20047	0.20049	210	1
12	0.29299	0.29296	1–21	7	29	0.19815	0.19808	0–32	4
13	0.27385	0.27396	−121	1	30	0.19407	0.19407	−212	5
14	0.25314	0.25308	−1–21	8	31	0.19152	0.1915	2–31	8
15	0.25136	0.25137	2–10	12	32	0.18938	0.18937	1–41	9
16	0.24391	0.24392	−211	14	33	0.18625	0.18621	−2–12	3
17	0.24020	0.24018	2–20	6	34	0.18417	0.18418	130	2

subjected to indexing. Calculated unite cell parameters are given in Table 3. Table 4 presents result of indexing of powder diffraction pattern of the triclinic β-Li_4WO_5 obtained in this work. Despite the fact that indexing results are in good agreement with literature data [15, 22] (Tables 1, 3) we turn our attention to powder diffraction pattern of high-temperature modification of Li_4WO_5, β-Li_4WO_5. Figure 1 shows fragments of powder diffraction patterns of orthorhombic Li_4WO_5 (generated on the basis of ICDD PDF 00-021-0530) (a), triclinic β-Li_4WO_5 obtained in this work (b) and triclinic Li_4WO_5 (generated on the basis of ICDD PDF 04-010-6772) (c). Analysis of the number of diffraction lines, their angular positions and relative intensities have revealed that diffraction pattern of triclinic β-Li_4WO_5 (Tables 1, 3) obtained by us is very similar to diffraction pattern of high-temperature orthorhombic modification of Li_4WO_5 [15] and differs to some extent from PDF 04-010-6772 calculated on the basis of structural data of β-Li_4WO_5 [22]. The differences consist in splitting or overlapping of certain pairs of reflections, like (−110)–(001), (110)–(−1−11) or (101)–(1−21) and measurable shift of diffraction lines on powder diffraction pattern of sample obtained by us towards lower 2θ angles. As a consequence of it, unit cell parameters of β-Li_4WO_5 obtained by us are somewhat larger than these presented by Hoffmann and Hoppe [22] (Tables 1, 3). The differences in unit cell parameters are responsible for splitting or overlapping of certain reflections. It is worth to mention that single crystal which was used in the structure solving of β-Li_4WO_5 was obtained by heating a mixture containing components in atomic ratio Li/W = 4.4:1 at 950 °C for 28 days in gold tube. It is possible that lithium content in single crystal of β-Li_4WO_5 obtained by Hoffmann and Hoppe [22] was higher than assumed (Li/W = 4:1) or that temperature of 950 °C is necessary for ordering of ions in the lithium and tungsten sublattices. To clarify this problem, sample of β-Li_4WO_5 obtained at 700 °C was additionally heated for 2 h at 1000 °C and next cooled to room temperature and subjected to XRD phase analysis. Figure 2 shows fragments of powder diffraction patterns of β-Li_4WO_5 recorded after heating stage at 700 °C (a) and after additional heating at 1000 °C for 2 h

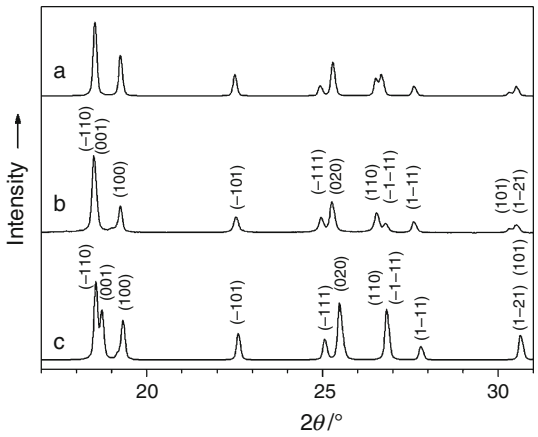

Fig. 1 Comparison of fragments of powder diffraction patterns of (*a*) orthorhombic Li_4WO_5 (generated on the basis of ICDD PDF 00-021-0530), (*b*) triclinic β-Li_4WO_5 obtained in this work and (*c*) triclinic Li_4WO_5 (generated on the basis of ICDD PDF 04-010-6772)

(b). Results of phase analysis have revealed that sample after additional heating at 1000 °C except the β-Li_4WO_5 contains also Li_2WO_4 and Li_2O. It is in accord with literature data informing that at 1100 °C β-Li_4WO_5 decomposes yielding Li_2WO_4 and Li_2O [15]. As there were no evidences of splitting and overlapping of reflections as a result of heating at 1000 °C, this problem requires further investigations.

The single-phase samples of Li_2WO_4, $Li_2W_2O_7$ and α-Li_4WO_5 obtained after heating stages at 650 °C as well as β-Li_4WO_5 obtained after heating stage at 700 °C were subjected to the DTA–TG investigation up to 1000 °C. Figure 3a shows DTA–TG curves of Li_2WO_4 and Fig. 3b DTA–TG curves of $Li_2W_2O_7$. On each DTA curve was recorded only one endothermic effect, with their onsets at 745 °C for Li_2WO_4 and 735 °C in the case of $Li_2W_2O_7$.

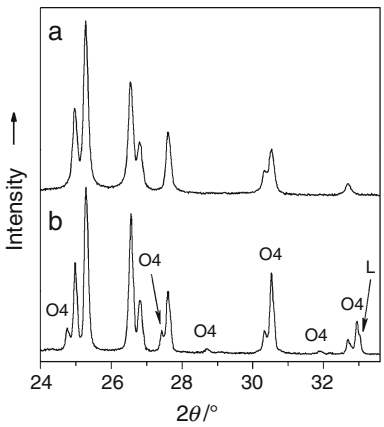

Fig. 2 Comparison of fragments of powder diffraction patterns of (*a*) β-Li_4WO_5 recorded after heating stage at 700 °C and after additional heating at 1000 °C for 2 h (*b*), where O4 stands for Li_2WO_4 and L stands for Li_2O

It was in accord with literature data where these endothermic effects were attributed to the melting of these phases [5–7, 11, 13, 14, 18]. TG curves of both phases did not contain any mass change effects. In order to explain melting behaviour of Li_2WO_4 and $Li_2W_2O_7$, samples of these compounds were additionally heated for 3 h at 780 °C, i.e., at temperature close to the extremum temperature of the endothermic effects registered on the DTA curves.

At temperature 780 °C, samples were liquid, colourless and transparent. After heating at 780 °C, samples were cooled rapidly to room temperature. The X-ray phase analysis of the melted and next quenched samples showed that they comprised only Li_2WO_4 and $Li_2W_2O_7$, respectively, which suggests congruent melting in both cases. On the other hand, Fig. 4 shows the DTA–TG curves of β-Li_4WO_5 (3a) and α-Li_4WO_5 (3b). On the DTA curve of α-Li_4WO_5 was recorded one small endothermic effect with onset temperature at 690 °C which was accompanied by small mass loss effect (2%). TG curve of α-Li_4WO_5 includes also another small mass loss effect (0.8%) with onset temperature at 230 °C, which was not accompanied by any thermal effects. The first mass loss effect the most probably can be attributed to desorption of water adsorbed by α-Li_4WO_5. The endothermic effect with onset at 690 °C can be connected with phase transition to β-Li_4WO_5. This is in accord with results of our XRD investigations (Table 2) indicating run of phase transition leading from α-Li_4WO_5 to β-Li_4WO_5 in the temperature range of 650–700 °C and literature data [7, 15]. However, the nature of the second mass loss effect is unknown and cannot be explained using only results of DTA–TG investigations. On the DTA curve of β-Li_4WO_5 was recorded only one endothermic effect with onset temperature at 210 °C, which was accompanied by small mass loss effect (2%). This mass loss effect was, however, greater than this

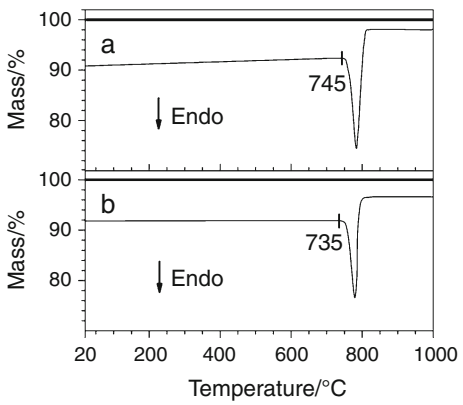

Fig. 3 DTA (*light line*) and TG (*dark line*) curves of pure: (*a*) Li_2WO_4 obtained after last heating stage at 650 °C and (*b*) $Li_2W_2O_7$ obtained after heating stage at 650 °C

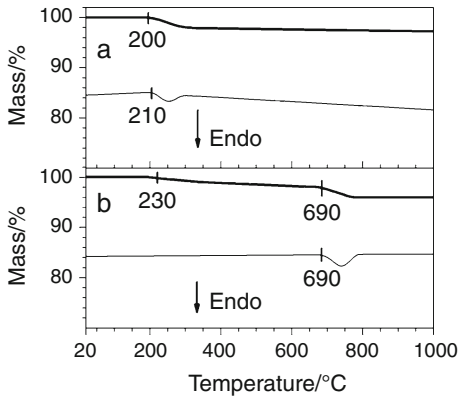

Fig. 4 DTA (*light line*) and TG (*dark line*) curves of pure: (*a*) β-Li_4WO_5 obtained after heating stage at 700 °C and (*b*) α-Li_4WO_5 obtained after heating stage at 650 °C

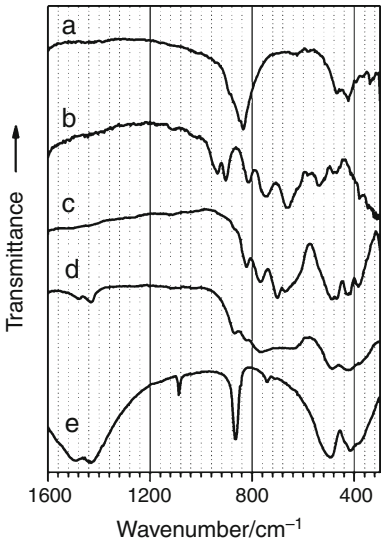

Fig. 5 IR spectra registered for pure samples obtained by the solid state reaction: (*a*) Li_2WO_4, (*b*) $Li_2W_2O_7$, (*c*) β-Li_4WO_5, (*d*) α-Li_4WO_5 and (*e*) Li_2CO_3

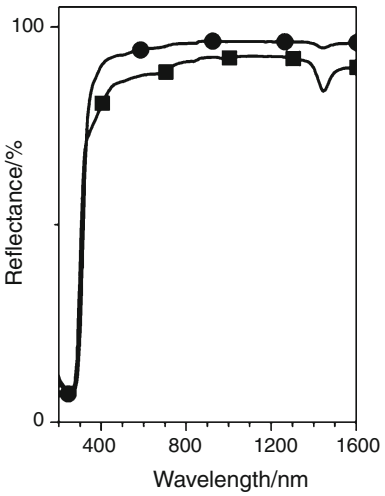

Fig. 6 UV–Vis–NIR/DRS spectra of α-Li_4WO_5 (*circle*), β-Li_4WO_5 (*square*)

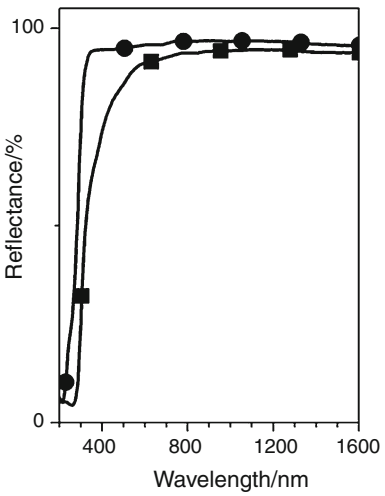

Fig. 7 UV–Vis–NIR/DRS spectra of $Li_2W_2O_7$ (*square*), Li_2WO_4 (*circle*)

recorded in the same temperature range on TG curve of α-Li_4WO_5. This effect can also be connected with desorption of water adsorbed, this time, by β-Li_4WO_5 (Fig. 4).

In order to know better properties of obtained phases and to explain the nature of mass loss effects recorded on TG curves of α-Li_4WO_5 and β-Li_4WO_5, single-phase samples of Li_2WO_4, $Li_2W_2O_7$, β-Li_4WO_5 and, α-Li_4WO_5 were subjected to an investigation with the help of IR and UV–Vis–NIR/DRS spectroscopy. Figure 5 shows the IR spectra of Li_2WO_4 (curve a), $Li_2W_2O_7$ (curve b), β-Li_4WO_5 (curve c), α-Li_4WO_5 (curve d) and for comparison Li_2CO_3 (curve e), Fig. 6 shows UV–Vis–NIR/DRS spectra of β-Li_4WO_5 (square) and α-Li_4WO_5 (circle), whereas Fig. 7 shows UV–Vis–NIR/DRS spectra of Li_2WO_4 (circle) and $Li_2W_2O_7$ (square).

Analysis of the number and positions of absorption bands recorded in the IR spectra of Li_2WO_4, $Li_2W_2O_7$, β-Li_4WO_5 and α-Li_4WO_5 phases obtained in this work has shown good agreement with literature data in the wavenumber range of 1000–400 cm^{-1} [7, 8]. However, analysis of IR spectra in the range of 1600–1000 cm^{-1}, not investigated earlier by other authors, has revealed in spectrum of α-Li_4WO_5 (Fig. 5, curve d) weak absorption bands with maxima at 1430 and 1480 cm^{-1}, characteristic for carbonates [31]. Similar bands, however much stronger, occur in IR spectrum of Li_2CO_3 (Fig. 5 curve e) but are

absent in the spectra of other investigated phases. Thus, from the analysis of the envelopes of recorded spectra shown in Fig. 5, let us come to conclusion that mass loss effect recorded at 690 °C on TG curve of α-Li_4WO_5 can be attributed to elimination of carbonate groups from the crystal lattice of this phase. We cannot exclude, however, that carbonate groups are eliminated from amorphous admixture accompanied α-Li_4WO_5, but not detectable by XRD. These both assumptions raise question concerning real composition of α-Li_4WO_5.

On the other hand, analysis of the UV–Vis–NIR/DRS spectra of α-Li_4WO_5 and β-Li_4WO_5 has shown that they contain weak absorption bands with maxima near 1430 nm, characteristic for water [24, 32]. Intensity of this band is higher in the case of β-Li_4WO_5. Such bands do not occur in the spectra of $Li_2W_2O_7$ and Li_2WO_4 (Fig. 7). It indicates that the small mass loss effects recoded on TG curves of α-Li_4WO_5 and β-Li_4WO_5 in the temperature range 200–230 °C can be connected with elimination of water during heating of these samples.

Based on recorded UV–Vis–NIR/DRS spectra and using procedures described in [33–35], band gap energy values for Li_2WO_4, $Li_2W_2O_7$, α-Li_4WO_5 and β-Li_4WO_5 equal to 4.35, 4.03, 4.00 and 4.12 eV, respectively, were calculated.

Conclusions

- Reinvestigations of the Li_2O–WO_3 system have been performed with the aid of DTA–TG, XRD, IR and UV–Vis–NIR/DRS measuring techniques and WO_3 and Li_2CO_3 as a reactants.
- Using applied procedure of synthesis, four single phases have been obtained: Li_2WO_4, $Li_2W_2O_7$, α-Li_4WO_5 and β-Li_4WO_5.
- Diffraction reflection characteristic for $Li_2W_5O_{16}$, $Li_2W_4O_{13}$ and $Li_6W_2O_9$ was identified on powder diffraction patterns of several samples, but it was not possible to obtain these compounds as single phases.
- Formation of Li_6WO_6 has not been corroborated in our research.
- Results of DTA–TG and XRD investigations have revealed that phases $Li_2W_2O_7$ and Li_2WO_4 melt congruently at 735 and 745 °C, respectively, whereas α-Li_4WO_5 undergoes a phase transition to β-Li_4WO_5 at 690 °C.
- Results of DTA–TG and IR investigations indicate that crystal structure of α-Li_4WO_5 can be stabilized by a small amount of carbonate groups.
- Based on UV–Vis–NIR/DRS investigations, band gap energies for Li_2WO_4, $Li_2W_2O_7$, α-Li_4WO_5 and, β-Li_4WO were calculated.

References

1. Prolong V, Venkatesh G, Malo S, Caignaert V, Baies R, Raveau B. Electrochemical synthesis of lithium-rich rock-salt-type oxide $Li_5W_2O_7$ with reversible deintercalation properties. Inorg Chem. 2014;53:522–7.
2. Singh DJ. Relationship of Li_2WO_4 to the scheelite tungstate scintillators: electronic structure and atomic positions from density-functional calculations. Phys Rev. 2008;B77:113101.
3. Nipan GD. Phase states of Li/W/Mn/SiO_2 composites in catalytic oxidative coupling of methane. Inorg Mater. 2015;51:389–95.
4. Lv P, Chen D, Li W, Xue L, Huang F, Liang J. Subsolidus phase relationships in the system ZnO–Li_2O–WO_3. J Alloys Compd. 2008;460:142–6.
5. Parmentier M, Reau JM, Fouassier C, Gleitzer C. Lithium polymolybdates and polytungstates. Bull Soc Chim Fr. 1972;5:1743–5.
6. Luke L, Chang Y, Sachdev S. Alkali tungstates: stability relations in the systems A_2O–WO_3–WO_3. J Am Ceram Soc. 1975;58:267–70.
7. Hauck J. Uranates(VI) and tungstates(VI) within the system Li_2O–UO_3–WO_3. J Inorg Nucl Chem. 1974;36:2291–8.
8. Kurilenko LN, Serebryakova NV, Saunin EI, Gromov VV, Sokolova NP. IR spectroscopy of the Li_2O–WO_3 and Li_2O–MoO_3 systems. Bull Acad Sci USSR. 1988;37:839–44.
9. Horiuchi H, Moriimoto N. The crystal structure of Li_2WO_4-II: a structure related to spinel. J Solid State Chem. 1979;30:129–35.
10. Waltersson K, Wilhelmi KA, Werner PE. The structure of Li_2WO_4 (IV). A high pressure polymorph of lithium wolframate. Cryst Struct Commun. 1977;6:225–30.
11. Pistorius CWFTJ. Phase behavior of Li2WO4 at high pressures and temperatures. Solid State Chem. 1975;13:325–9.
12. Yamaoka S, Fukunaga O, Ono T, Tizuka E, Asami S. Phase transformations in Li_2WO_4 at high pressure. J Solid State Chem. 1973;6:280–5.
13. Hartmann P. A uniform description of phenakite type structures as superstructures of beta-Si_3N_4. Z Kristallogr. 1989;187:139–44.
14. Drobasheva TI, Bogoduhova NA, Buhalova GA. Li_2WO_4–Na_2WO_4–WO_3 system. Zh Neorg Khim. 1975;20:3097–102.
15. Reau JM, Fouassier C, Hagenmuller P. New oxygen phases in ternary system A_2O–MO_3 of formulas A_4MO_5 and A_6MO_6 (A = Li, Na; M = Mo, W). Bull Soc Chim Fr. 1967;680:3873–6.
16. Hauck J. Zur Kristallstruktur des Li_6WO_6. Z Naturf. 1969;B24:251.
17. Parmentier M, Gleitzer C, Aubry J, Chaudron MG. Un tungstate basique de lithium Li_6WO_6. A basic lithium tungstate $Li_6W_2O_9$. C R Seances Acad Sci. 1972;274:1681–3.
18. Reau MJ, Fouassier C. Les systemes MO_3–A_2O (M = Mo, W; A = Li, Na, K). Bull Soc Chim Fr. 1971;2:398–402.
19. Okada K, Morikawa H, Marumo F, Iwai S. The crystal structure of $Li_2W_2O_7$. Acta Cryst. 1975;31:1451–5.
20. Blasse G. On the structure of some compounds $Li_3Me^{5+}O_4$ and some other mixed metal oxides containing Lithium. Z Anorg Allg Chem. 1964;331:44–50.
21. Wilhelmi KA, Waltersson K, Lofgren P. On the structure of a high pressure polymorph of lithium wolframate(VI), Li_2WO_4(-III). Cryst Struct Commun. 1977;6:219–25.

22. Hoffmann R, Hoppe R. Two new order variations of NaCl-type: Li_4MoO_5 and Li_4WO_5. Z Anorg Allg Chem. 1989;573:157–69.
23. Piątkowska M, Tomaszewicz E. Synthesis, structure, and thermal stability of new scheelite-type $Pb_{1-3x}\square_xPr_{2x}(MoO_4)_{1-3x}(WO_4)_{3x}$ ceramic materials. J Therm Anal Calorim. 2016;126:111–9.
24. Tabero P, Frackowiak A. Synthesis of $Fe_8V_{10}W_{16}O_{85}$ by a solution method. J Therm Anal Calorim. 2016;125:1445–51.
25. Tabero P. Formation and properties of the $Fe_8V_{10}W_{16-x}Mo_xO_{85}$ type solid solution. J Therm Anal Calorim. 2007;88:37–41.
26. Bosacka M, Filipek E, Paczesna A. Unknown phase equilibria in the ternary oxide V_2O_5–CuO–In_2O_3 system in subsolidus area. J Therm Anal Calorim. 2016;125:1161–70.
27. Checmanowski J, Pelczarska AJ, Szczygiel I, Szczygiel B. Influence of ceria and yttria on the protective properties of SiO_2–Al_2O_3 coatings deposited by sol–gel method on FeCrAl alloy. J Therm Anal Calorim. 2016;126:371–80.
28. Souza MT, Cesconeto FR, Arcaro S, Teixeira AHB, Raupp-Pereira F, Montedo ORK, Novaes de Oliveira AP. Synthesis and characterization of Li_2TiSiO_5 obtained by melting and solid-state reaction. J Therm Anal Calorim. 2017;127:463–7.
29. Świderski G, Lewandowska H, Świsłocka R, Wojtulewski S, Siergiejczyk L, Wilczewska A. Thermal, spectroscopic (IR, Raman, NMR) and theoretical (DFT) studies of alkali metal complexes with pyrazinecarboxylate and 2,3-pyrazinedicarboxylate ligands. J Therm Anal Calorim. 2016;126:205–24.
30. Gorodylova N, Kosinová V, Dohnalová Ž, Šulcová P, Bělina P. Thermal stability and colour properties of $CuZr_4(PO_4)_6$. J Therm Anal Calorim. 2016;126:121–8.
31. Gadsen JA. Infrared spectra of minerals and related inorganic compounds. London: Butterworths; 1975.
32. Gabrus E, Nastaj J, Tabero P, Aleksandrzak T. Experimental studies on 3A and 4A zeolite molecular sieves regeneration in TSA process: aliphatic alcohols dewatering-water desorption. Chem Eng J. 2015;259:232–42.
33. Kim K, Park JH, Kim H, Kim JK, Schubert EF, Cho J. Energy bandgap variation in oblique angle-deposited indium tin oxide. Appl Phys Lett. 2016;108(041910):1–4.
34. Joseph P, Petchimuthu K, Chinnapiyan V. Enhanced band gap energy and electrochromic behaviour of selenium incorporated copper thin film. J Phys Sci. 2016;27:41–54.
35. Liu P, Longo P, Zaslavsky A, Pacifici D. Optical bandgap of single- and multi-layered amorphous germanium ultra-thin films. J Appl Phys. 2016;119(014304):1–9.